Phytomedicine 143 (2025) 156913

Contents lists available at ScienceDirect

Phytomedicine

journal homepage: www.elsevier.com/locate/phymed

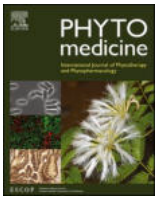

Original Article

Mechanism of Dihydroartemisinin in activating macrophages to enhance host resistance to malaria

Xin Li [a,b,1], Qilong Li [a,b,1], Ning Jiang [a,b,1], Kexin Zheng [a,b], Yiwei Zhang [a,b], Xiaoyu Sang [a,b], Ying Feng [a,b], Ran Chen [a,b], Qijun Chen [a,b,*]

[a] Key Laboratory of Livestock Infectious Diseases, Ministry of Education, and Key Laboratory of Ruminant Infectious Disease Prevention and Control (East), Ministry of Agriculture and Rural Affairs, College of Animal Science and Veterinary Medicine, Shenyang Agricultural University, 120 Dongling Road, Shenyang 110866, PR China
[b] Research Unit for Pathogenic Mechanisms of Zoonotic Parasites, Chinese Academy of Medical Sciences, 120 Dongling Road, Shenyang 110866, PR China

ARTICLE INFO

Keywords:
Dihydroartemisinin
Immunoregulation
Macrophage
Malaria
Plasmodium

ABSTRACT

Background: The property of dihydroartemisinin (DHA) in promoting host immunohomeostasis, apart from its potent antimalarial activity, has been well-recognized. However, the mechanism of DHA in activating macrophages to enhance host resistance to malaria remains unexplored.
Purpose: This study investigated the molecular mechanism by which DHA promotes the polarization of macrophages toward the M1 phenotype during the treatment of malaria.
Methods: The mouse macrophage cell line RAW 264.7 or the macrophages isolated from mice were stimulated with *Plasmodium berghei* ANKA infected red blood cells (iRBC) in the presence of DHA. The macrophage phenotypes in both *in vivo* and *in vitro* were determined using cytometric bead array and flow cytometry. To dissect the molecular mechanisms underlying macrophage responses to DHA, we initially profiled the expression of 90 genes associated with innate immunity, including the entire NLR family, in macrophages stimulated with DHA. This targeted screen strikingly revealed that only *Nlrp12* was significantly upregulated among all tested NLR genes. The function of *Nlrp12* was further dissected by *Nlrp12* knockdown in macrophages with recombinant lentiviruses encoding *Nlrp12*-specific shRNA, within the context of DHA treatment. To comprehensively define the molecular consequences of *Nlrp12* deficiency, we performed an integrated analysis by combining single-cell RNA sequencing with label-free quantitative proteomic profiling. This allowed us to systematically characterize the complex transcriptomic and proteomic dynamics in DHA-treated macrophages upon *Nlrp12* deletion.
Results: DHA induced macrophage polarization to M1 phenotype and enhanced phagocytosis by up-regulating the expression of NLRP12. *Nlrp12*-knockdown in macrophages reduced the expression of M1 type-associated genes, resulting in a significantly increased expression of the translocator protein (TSPO), which suppressed the secretion of inflammation-associated cytokines and blunting macrophage M1 polarization. The results of

Abbreviations: Acp5, Acid Phosphatase 5; ACT, Artemisinin-based combination therapy; AIM2, absent in melanoma 2; Alox, Arachidonate Lipoxygenase; Angptl6, Angiopoietin Like 6; Arg1, Arginase 1; Avil, Advillin; Bid, BH3 Interacting Domain Death Agonist; Car6, Carbonic Anhydrase; CARD, caspase recruitment domain; Cdca8, Cell Division Cycle Associated 8; Cenpf, Centromere Protein F; Cox6a2, Cytochrome C Oxidase Subunit 6A2; Cxcl2, C-X-C Motif Chemokine Ligand 2; DEGs, differentially expressed genes; DEPs, differentially expressed proteins; DHA, dihydroartemisinin; Fcgr1, Fc gamma RI; Fyco1, FYVE And Coiled-Coil Domain Autophagy Adaptor 1; Gapdh, Glyceraldehyde-3-Phosphate Dehydrogenase; GBP5, Guanylate Binding Protein 5; Gm26917, Predicted Gene, 26917; Hcst, Hematopoietic Cell Signal Transducer; Hist1h2bb, Histone Cluster 1 H2B Family Member B; Ifi202b, Encoding For the P202b Protein; Ifitm3, Interferon Induced Transmembrane Protein 3; IFN-?, Interferon-?; IL-1ß, interleukin-1 beta; Il1rn, Interleukin 1 Receptor Antagonist; iNOS, inducible nitric oxide synthase; Jup, Junction Plakoglobin; Lcn2, Lipocalin-2; MCP-1, Monocyte chemoattractant protein-1; MFI, median fluorescence intensity; Naip1, NLR Family Apoptosis Inhibitory Protein; NLRP3, NOD-, LRR- and pyrin domain-containing protein 3; NLRP12, NLR Pyrin Domain Containing 12; Nme2, NME/NM23 Nucleoside Diphosphate Kinase 2; Nod1, Nucleotide Binding Oligomerization Domain Containing 1; PAMPs, pathogen-associated molecular patterns; Plk1, Polo Like Kinase 1; Prc1, Protein Regulator Of Cytokinesis 1; Prdx1, Peroxiredoxin 1; PRRs, pattern recognition receptors; Pttg1, Pituitary Tumor Transforming Gene 1; Rnf183, Ring Finger Protein 183; Sh2d6, SH2 Domain Containing 6; Snhg5, Small Nucleolar RNA Host Gene 5; Spp1, Secreted Phosphoprotein 1; TGF-ß, Transforming Growth Factor Beta; TNF-a, tumor necrosis factor-a; TSPO, translocator protein; Tubb4bm, Tubulin Beta 4B Class IVb; Ube2c, Ubiquitin Conjugating Enzyme E2 C; UMAP, Uniform Manifold Approximation and Projection; Ung, Uracil DNA Glycosylase.

* Corresponding author.
E-mail address: qijunchen759@syau.edu.cn (Q. Chen).
[1] These authors contributed equally.

https://doi.org/10.1016/j.phymed.2025.156913
Received 2 July 2024; Received in revised form 21 May 2025; Accepted 26 May 2025
Available online 26 May 2025

single cell RNA sequencing further revealed that DHA promoted the conversion of classical M1 macrophages into lipocalin-2 (Lcn2) ^{high} M1 macrophages.
Conclusion: The activation of *NLRP12* induced by DHA is crucial for M1 macrophage polarization, which plays a significant role in the clearance of *Plasmodium* parasites.

Introduction

In 2022, an estimated 249 million clinical malaria cases and 608,000 malaria-related deaths were reported worldwide (Venkatesan, 2024). One of the typical clinical symptoms of malarial attacks is undulant fever, which is the result of excessive cytokine release from immune cells, including interleukin-1 beta (IL-1β), tumor necrosis factor-α (TNF-α), and IL-12 (Gazzinelli et al., 2014). High levels of IL-1β chemotactically direct macrophages to the site of inflammation, which subsequently release more IL-1β, being strongly associated with disease severity and death (Caronni et al., 2023). In malaria, the *Plasmodium* parasite can drive macrophage differentiation toward M2 phenotype, rather than M1 phenotype, which is closely associated with parasite escape from immune clearance (Kapralov et al., 2020).

Artemisinin-based combination therapy (ACT) remains an effective approach in malaria treatment (Venkatesan, 2024) with dihydroartemisinin (DHA)-piperaquine as the most used ACT (Wallender et al., 2021). DHA can directly kill *Plasmodium* parasites both *in vivo* and *in vitro* (Asahi et al., 2023; Gibbons et al., 2007). In addition to its antimalarial effect, DHA has been shown to promote T cell activity, suppress Th_2 responses and M2-type marker expression on macrophages (Li et al., 2022). However, the underlying molecular mechanism remains unclear.

Inflammasomes are polyprotein complexes that are formed in the cytoplasm of macrophages in response to microbial molecules or stress signals. These complexes include pattern recognition receptors (PRRs), adapters, and inflammatory caspases (Schroder and Tschopp, 2010). During *Plasmodium* infection, macrophages sense their surroundings through PRRs that detect *Plasmodium*-specific pathogen-associated molecular patterns (PAMPs), such as pigments, which are by-products of hemoglobulin metabolism during intraerythrocytic development of *Plasmodium* parasites. This detection initiates inflammasome assembly, leading to the release of various inflammatory mediators (Coban et al., 2005). Inflammasome activation involves the activation of caspase-1 and the production of mature IL-1β and IL-18, which can trigger inflammation and cell death (Guo et al., 2015). Haemozoin is crucial for activating the NOD-, LRR- and pyrin domain-containing protein 3 (NLRP3), absent in melanoma 2 (AIM2), and type I interferon responses (Kalantari et al., 2014). Thus, targeting NLRP3 and AIM2 inflammasome activity may offer therapeutic benefits (Kalantari et al., 2014). *Plasmodium* DNAs can also trigger the assembly of the inflammasome including the apoptosis-associated speck-like protein containing a caspase recruitment domain (CARD), NLRP3, and NLRP12, which results in caspase-1 activation and subsequent production of IL-1β following secondary activation of Toll-like receptors (Pereira et al., 2020). Additionally, previous studies indicated that elevated expression of the inflammasome NLRP3 in macrophages promotes M1 polarization, while inhibition of NLRP3 led to polarization toward the M2 phenotype (Jiao et al., 2021; Liu et al., 2021). It is, however, unknown whether DHA treatment in malaria patients will influence NLRPs expression and the fate of macrophages.

Materials and methods

Medication preparation

For experiments *in vivo*, 0.15 g of carboxymethyl cellulose (CMC, Solarbio Company, Beijing, China, Catalog No 9004–32–4) was dissolved in 30 ml of warm distilled water. When the temperature of the solution reaches 25 °C, 0.3 g DHA (Aladdin Biochemical Technology *Co. Ld*, China, Catalog No 3000,518, ~98 % purity) was added to the CMC solution, followed by stirring for 24 h in dark as described (Li et al., 2022). CMC without DHA was used as solvent control.

For experiments *in vitro*, 28.4 mg of DHA was added to 10 ml of ethanol (Tianjin Zhongtian Chemical Co., Ltd., Tianjin, China, CAS No.64–17–5), and after it was fully dissolved, 10 μl of the solution was added to 990 μl of phosphate-buffered saline (PBS) to make a 100 μM DHA solution. In the control group,10 μl of ethanol solution was added to 990 μl of PBS to make 170 μM ethanol solution.

Animals

Female C57BL/6 mice ($n = 120$), aged 6 to 8 weeks, were purchased from Liaoning Chang Sheng Biological Technology Company (Benxi, Liaoning, China) and maintained in a specific pathogen-free facility with free access to food and water. All procedures involving experimental animals were conducted following the Animal Husbandry Guidelines of Shenyang Agricultural University, and all animal experiments were approved by the ethics committee of Shenyang Agricultural University (Ethical Clearance Permission No SYXK < Liao>2021–0010).

Passage of blood-stage Plasmodium berghei ANKA

The parasite *P. berghei* ANKA strain was maintained by frequent infection in C57/BL6 mice. Briefly, mice were inoculated intraperitoneally with 0.2 ml of infected blood. Three days after the first infection, the parasitemia was counted after staining with 10 % Giemsa stain (Beyotime, Shanghai, China, C0133–100 ml) for 15 min at room temperature. The parasitemia was monitored daily *via* microscopy.

Cultivation of murine macrophages and the human embryonic kidney 293T cell line

Murine-derived macrophage cells (RAW264.7) were cultured in RPMI-1640 medium (HyClone, Waltham, MA, USA, SH30255.01), and the human embryonic kidney 293T cells were cultured in Minimum Essential Medium (HyClone, SH30024.01). Both media were supplemented with 10 % fetal bovine serum (FBS; Gibco, Grand Island, NY, USA, 10099141C) and 0.5 % Penicillin-Streptomycin Solution (100X) (Beyotime, C0222). Briefly, the frozen cells were thawed in a 37 °C water bath, inoculated into 6-cm culture dishes, and cultured overnight. The non-adherent cells were washed away with medium. The cell cultures were maintained until 80 % confluency. The cultures were regularly tested for free of mycoplasma contamination.

Detection of macrophage phagocytosis

RAW264.7 cells were cultured on coverslips in the wells of culture plates as described in the previous section. Infected red blood cells (iRBC) were separated from the peripheral blood of *P. berghei* ANKA-Infected mice using Percoll density gradient centrifugation and resuspended in RPMI-1640 medium.

RAW264.7 cells were seeded onto cell-coated coverslips and cultured in 6-well plates as above. The cells were divided into the following groups ($n = 3$ biological replicates *per* group, as illustrated in Supplementary Fig. 1): (i) LPS: To induce M1 polarization, RAW264.7 cells were stimulated with LPS (100 ng/ml; Sigma-Aldrich, Cat# L2880) for 4 h following established protocols, serving as the positive control for M1

macrophage characterization (Orecchioni et al., 2019); (ii) Negative Control: RAW264.7 cells were incubated with 2×10^6 iRBCs for 24 h with DHA solvent; and (iii) DHA Treatment Groups: RAW264.7 cells were co-incubated with 2×10^6 iRBCs for 12 h and then incubated with DHA (200, 700 or 1600 nM) for 12 h. After that, iRBCs that did not adhere firmly to the RAW264.7 cells were washed away with PBS.

To further test the phagocytic effect of polarized M1 type macrophages after DHA treatment, the RAW264.7 cells in all groups were stained with 5 μM 3,3′-dioctadecyloxacarbocyanine perchlorate (DiO, Beyotime, C1993S) for 1 h. Meanwhile, 1×10^5 iRBCs, which had also been stained with 700 ng/ml dihydroethidium (DHE, Beyotime, S0063) for 1 h, were added to each group and incubated for 30 min. After that, iRBCs that did not adhere firmly to the RAW264.7 cells were washed away with PBS. Phagocytosed iRBCs were observed *via* a Spinning Disk Confocal and Structured Illumination joint Super-Resolution Microscope (SIM-ultimate, CSR Biotech Co., Ltd., Guangzhou; China).

PCR array screening of differentially expressed NLRPs

RAW264.7 cells incubated with 2×10^6 iRBCs for 24 h and that first incubated with 2×10^6 iRBCs for 12 h and then incubated with 700 nM DHA for 12 h were lysed on ice with 1 ml TRIzol reagent (Invitrogen, Carlsbad, *CA*, USA, 15,596,018), mixed with 0.2 ml of chloroform (Fuyu Chemical, Tianjin, China, 67–66–3). The mixture was shaken vigorously, allowed to stand at 25 °C for 10 min, and centrifuged at 12,000 g for 10 min at 4 °C. The water phase from each tube was aspirated and mixed with 0.5 ml of isopropanol (Fuyu Chemical, 67–63–0). The samples were allowed to stand at 25 °C for 10 min, followed by centrifugation at 12,000 g for 10 min at 4 °C. After removing the supernatant, the RNA pellets were washed twice with 75 % ethanol. The mRNAs were reverse-transcribed into cDNAs using a first-strand cDNA synthesis kit (Takara, Tokyo, Japan, 6210A). To determine the transcription levels of the 90 NLRPs, inflammasome PCR Array plates (Wcgene Biotech, Shanghai, China, WC-MRNA0078-M) were employed according to the manufacturer's protocols and subsequently verified *via* qPCR.

Construction of recombinant lentiviruses expressing NLRP12-specific shRNA

Three siRNA sequences including *mNLRP12* si-1 to 3, targeting the mRNA transcript of mouse *Nlrp12* gene (GenBank Accession Number NM_001033431.1) were designed (Supplementary Table 1) and preliminarily tested for their inhibitory effect on *Nlrp12* expression. The sequence of *mNLRP12* si-3 was eventually selected for further experiments. The shRNA cassette and its complementary strand were designed containing *AgeI* and *EcoRI* restriction sites (Supplementary Table 1). The shRNA-sequence was inserted into the pLKO.1-LUC-Puro lentiviral vector (Pavibio, Wuhan, China) to construct the recombinant vector pLKO.1-LUC- puromycin-*Nlrp12*-shRNA. The accuracy of the recombinant vector sequence was determined by sequencing. The recombinant lentiviruses with the *mNLRP12* si-3 targeting sequence and the negative control lentivirus without NLRP12 insert were termed shNlrp12 and shCtrl, respectively. A mixture of shNlrp12 and the packaging plasmid pHelper 1 (Hunan Fenghui Biotechnology Co., Ltd, Hunan, China, BR417) or shCtrl and the packaging plasmid pHelper 1 was respectively dissolved in serum-free RPMI-1640 medium with Lipofectamine 3000 (Invitrogen, L3000001) and co-transfected into the 293T cells. Puromycin with 3 μg/ml final concentration was added to the culture 48 h after transfection, and culture was continued for 72 h. The recombinant lentivirus titers were tested and set to 2×10^8 titer units (TUs)/ml.

shRNA-mediated Nlrp12 knockdown in RAW264.7 cells and mice

RAW264.7 cells were cultivated as described above. When the cell confluency reached 50–60 %, the recombinant lentiviruses, shNlrp12 and shCtrl, were respectively added to the cells in culture plates (multiplicities of infection=40 and 10, respectively) for 24 h before being removed and medium replaced. Lentivirus-infected cells were selected by the addition of the medium containing 500 ng/ml puromycin for 7 days.

For shRNA mediated *Nlrp12* knockdown in mice, the recombinant lentiviruses, shNlrp12 and shCtrl (1×10^7 TU/ *per* mouse), were injected into mice ($n = 8$ per group) *via* the tail vein. The expression of *Nlrp12* in the splenic cells of the mice were validated by qRT-PCR.

shRNA-mediated overexpression of the TSPO gene in RAW264.7 cells

A recombinant lentivirus that can over-express *Tspo* (designated Tspo-EO) and the control virus (designated Ctrl-EO) were purchased from HaiXing Bio, Suzhou, China. The RAW264.7 macrophages at 50–60 % confluence were inoculated with the Tspo-EO or Ctrl-EO recombinant lentiviruses at a multiplicity of infection (MOI) of 100. Following a 24-hour incubation, the medium was removed and replaced with fresh complete culture medium. Transfected cells were subsequently selected by culturing in a medium containing 500 ng/ml puromycin for 7 days.

Detection of macrophage polarization in vivo and in vitro by flow cytometry

RAW264.7 cells were divided into eleven experimental groups, as follows: (i) Negative control group: RAW264.7 cells treated with 170 μM ethanol solution for 12 h; (ii) LPS group: RAW264.7 cells incubated with 100 ng/ml LPS for 4 h to induce macrophage activation; (iii) iRBC group: RAW264.7 cells were incubated with *P. berghei* iRBCs (RAW264.7:iRBC=1:10) for 24 h; (iv) iRBC+DHA group: RAW264.7 cells were incubated with iRBCs for 12 h before addition of DHA (200, 700 or 1600 nM) to each well and continuing cultivation for 12 h; (v) shNlrp12 + iRBC + DHA group: RAW264.7 cells infected with shNlrp12 lentivirus, incubated with iRBCs for 12 h, then treated with 700 nM DHA for 12 h; (vi) shCtrl + iRBC + DHA group: RAW264.7 cells infected with shCtrl lentivirus, incubated with iRBCs for 12 h, then treated with 700 nM DHA for 12 h; (vii) DHA group: RAW264.7 cells respectively treated with DHA at concentrations of 200, 500, 700, 900, and 1600 nM, or 170 μM ethanol, or complete RPMI-1640 medium for 12 h; (viii) shNlrp12 + DHA + inhibit-TSPO group: RAW264.7 cells infected with shNlrp12 lentivirus, treated with 700 nM DHA for 12 h, then incubated with TSPO inhibitor (ONO-2952, MedChemExpress, Monmouth Junction, NJ, USA) for 2 h; (viiii) shNlrp12 + DHA control group: RAW264.7 cells infected with shNlrp12 lentivirus, treated with 700 nM DHA for 12 h; (x) Tspo-EO group: RAW264.7 cells infected with Tspo-EO lentivirus, treated with 700 nM DHA for 12 h; (xi) Ctrl-EO group: RAW264.7 cells infected with Ctrl-EO lentivirus, treated with 700 nM DHA for 12 h.

For analysis of the effect of DHA on macrophage phenotype shift, cells from the above eleven groups were de-attached from the wells and diluted into 1×10^7 cells/ml. About 1×10^6 cells in each group were pre-incubated with a purified anti-mouse CD16/32 (BioLegend, San Diego, *CA*, USA, 101,310) at 4 °C for 15 min to block nonspecific immunoglobulin binding to the Fc receptors. M1 macrophages were determined by respectively incubation with surface marker specific antibodies including anti-CD45, anti-CD11b, anti-F4/80 and anti-CD86 (Supplementary Table 2) at 4 °C for 30 min, followed by incubation with fluorophore-conjugated secondary antibodies (Supplementary Table 2). For determination of M2 macrophages, the cells were, at the first step, stained with the anti-CD45, anti-CD11b and anti-F4/80 antibodies in a same way as that for M1 type determination, followed by fixation, permeabilized with Cyto-Fast Fix/Perm Buffer (BioLegend), and stained with the anti-CD206 antibody, which were further incubated with a fluorophore-conjugated secondary antibody (Supplementary Table 2). The samples were analyzed using a fluorescence-activated cell sorting Aria III flow cytometer (BD Biosciences, San Jose, *CA*, USA).

To detect the macrophage polarization *in vivo*, splenic cells were

collected from seven mouse groups ($n = 8$ *per* group) as follows: (i) DHA treatment post-infection group: Mice were infected with *P. berghei* ANKA for 12 h, followed by orally administration with 2 mg DHA for 2 days; (ii) Vehicle control (Healthy + CMC) group: healthy mice received CMC treatment with the same volume of that of DHA; (iii) DHA treatment (Healthy) group: Healthy mice only treated with the same amount of DHA as above; (iv) Infection control group: *P. berghei* ANKA-infected mice received the same volume of CMC treatment as that of DHA; (v) shNlrp12 lentivirus infection group: Mice were intravenously injected with the recombinant shNlrp12 lentiviruses; (vi) shCtrl lentivirus infection group: Mice were injected with the shCtrl control viruses. (vii) LPS treatment group: Mice were injected intraperitoneally with 20 mg/ml of LPS, and the experiment was conducted 24 h later. The dosage of DHA was determined based on previous study (Zhang et al., 2020).

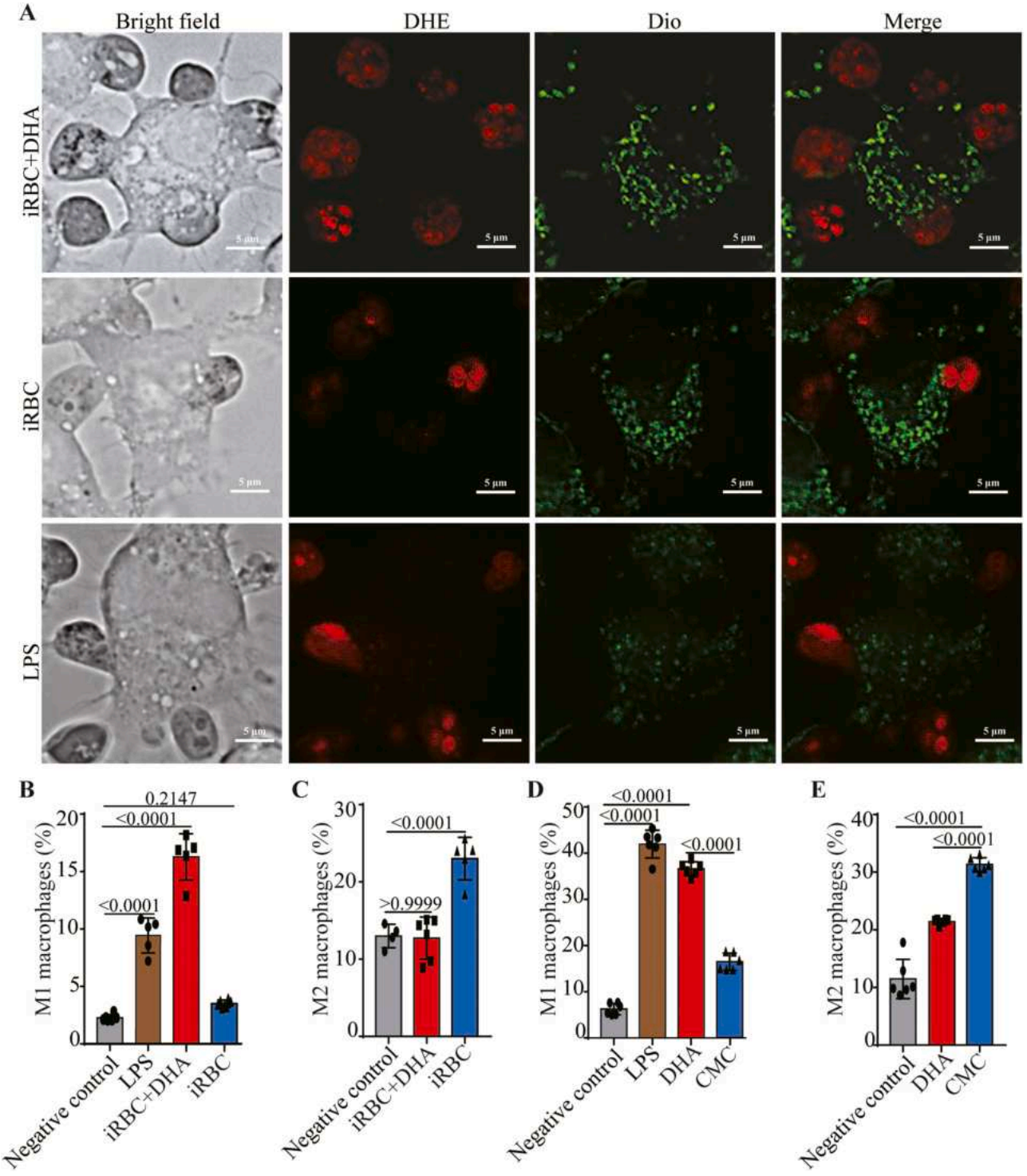

Fig. 1. DHA drives M1 polarization and phagocytosis of macrophages **(A)** Fluorescent labelled of iRBCs (red) phagocytosed by macrophages in different treatment groups. **(B, C)** Polarization of macrophages toward M1 and M2 phenotypes in different treatment groups. **(D, E)** *In vivo* analysis of macrophage polarization toward M1 and M2 phenotypes in mice after DHA treatment relative to the LPS or the untreated controls. Data represent the mean ± S.E.M., $n \geq 3$. DHA, dihydroartemisinin; DHE, dihydroethidium; DiO, dioctadecyloxacarbocyanine perchlorate; iRBC, infected red blood cells; LPS, Lipopolysaccharide.

After treatment, the splenic cells in all groups were processed through a 70-μm cell strainer and RBCs were removed using the red blood cell lysis buffer (BioLegend, Cat. No 420,301) to prepare single-cell suspensions. The experimental procedure for detection of macrophage polarization was the same as that with the cultivated cell lines described above.

Single-cell RNA sequencing

M1 macrophages separated from RAW264.7 cells following treatment with 700 nM DHA and the ethanol solvent control groups were subjected to trypan blue staining at a ratio of 9:1. Cell counting was performed using a conventional optical microscope and a hemocytometer, ensuring a viability of over 90 % and a cell concentration of at least 1000 cells/μl. Single-cell RNA-seq libraries were prepared using 10x Genomics v3.1 chemistry according to standard protocols. Initially, the kits were utilized to generate a single-cell Gel Beads-in-Emulsion (GEM), followed by post-GEM-RT cleanup, barcoding, cDNA amplification, and construction of the cDNA libraries. These libraries were sequenced on an Illumina NovaSeq 6000 platform. Each group included three biological replicates, forming six cDNA libraries (three from the DHA and control groups).

Statistical analysis

All analyses were performed using the GraphPad Prism 7 software (GraphPad Software Inc., La Jolla, *CA*, USA). The results were analyzed using a two-tailed Student's T-test or analysis of variance when multiple groups were compared. Results were expressed as the mean ± *S*.E.M. Statistical significance was set at $p < 0.05$. Cytokine levels were represented using the FCAP Array Software (v3.0; BD Biosciences). The applied software is listed in the Supporting Information (Supplementary Table 3). Uncropped blots are found in Supplementary Figures 2.

Results

DHA enhanced macrophage phagocytosis and M1 polarization

We first assessed the cytotoxicity of DHA on macrophages. DHA concentrations up to 700 nM did not induce cytotoxic effects in RAW264.7 macrophages (Supplementary Fig. 3A). This concentration is physiologically relevant, falling within the peak serum levels observed in malaria patients treated with DHA (White, 2008), and was therefore selected for subsequent experiments. Notably, DHA treatment significantly enhanced the phagocytic ability of RAW264.7 macrophages compared to the solvent control (Fig. 1A; Videos 1, 2). Furthermore, 700 nM DHA increased macrophage phagocytosis to a greater extent than the LPS positive control (Fig. 1A). These findings collectively demonstrate that DHA enhances the phagocytic activity of macrophages towards iRBCs.

Treatment of macrophages with various concentrations of DHA (from 200 to 1600 nM), or macrophages incubated with iRBCs followed by treatment with DHA, resulting in an increase in M1 type macrophages, with 700 nM DHA causing a more significant M1 polarization compared to the control (Supplementary Fig. 3B, C). In contrast, RAW264.7 macrophages only incubated with iRBCs differentiated towards the M2 phenotype (Fig. 1B, C). However, upon the addition of DHA, RAW264.7 macrophages polarized towards the M1 phenotype (Fig. 1B, C). Importantly, the findings with the RAW264.7 macrophage cell line were also confirmed with splenic macrophages from mice treated in the same approach (Fig. 1D, E). Overall, these findings indicated that DHA enforced macrophage phagocytosis and M1 polarization, which likely promoted the clearance of *Plasmodium* parasites.

The expression of NLRP12 was upregulated in macrophages under DHA treatment

The activation of the *NLRP* is crucial for maintaining macrophage polarization (Rao et al., 2022a). To elucidate the molecular mechanisms underlying DHA-driven M1 polarization in macrophages, we first performed a PCR array screening for the transcription of 90 NLRPs in both DHA-treated and control macrophages. Our results showed that DHA treatment significantly upregulated the expression of *Nlrp12, Nlrp6*, and *Nlrp1a*, while downregulating *Nlrp4e*, NLR family apoptosis inhibitory protein (*Naip1*), *AIM2*, and nucleotide binding oligomerization domain containing 1 (*Nod1*) (Fig. 2A). Subsequently, we verified the transcription and protein expression of these candidate genes in macrophages using qPCR and Western blot. These analyses confirmed that only NLRP12 was consistently upregulated in DHA-treated macrophages compared to controls, at both transcriptional and protein levels (Fig. 2B-D; Supplementary Fig. 3D). Furthermore, molecular docking analysis revealed hydrogen bond interactions between DHA and the NLRP12 protein, with a docking score of −7.3 kcal/mol (Supplementary Fig. 4A). Consistent with NLRP inflammasome activation, we observed significantly increased expression levels of mature IL-1β protein, a key downstream effector, under DHA treatment (Supplementary Fig. 4B, C). This indicates that the NLRPs are activated and functional in this context (Sundaram et al., 2023). These findings suggest that DHA-induced macrophage M1 polarization is likely associated with NLRP12 expression.

NLRP12 expression is closely associated with DHA-induced M1 macrophage polarization

To validate the functional role of *Nlrp12* in DHA-driven M1 polarization, stable *Nlrp12*-knockdown cell lines were established by infection of macrophages with recombinant lentiviruses expressing *Nlrp12*-specific shRNA (shNlrp12), followed by phenotypic verification (Supplementary Fig. 5). The successful knockdown of the *Nlrp12* transcripts in macrophages was confirmed by qPCR, and these results showed that *Nlrp12* expression was significantly reduced in the macrophages infected with the lentivirus shNlrp12 (Supplementary Fig. 6A).

In *Nlrp12*-knockdown macrophages, DHA treatment not only resulted in weakened phagocytosis but also significantly reduced the proportion of M1 macrophages compared to the control group (Fig. 3A-C). These findings suggest that *Nlrp12* is a key regulator in DHA-induced macrophage M1 polarization. To verify whether *Nlrp12* also mediates DHA-induced macrophage M1 polarization *in vivo, Nlrp12*-knockdown mice were successfully generated (Supplementary Fig. 6B). Consistent with our *in vitro* results (Fig. 3B, C), the reduction of *Nlrp12* expression resulted in a significant decrease in the proportion of M1 macrophages in *P. berghei* ANKA-Infected mice (*Nlrp12*-knockdown background) treated with DHA (Fig. 3D, E). Thus, these results indicate that DHA could stimulate NLRP12 expression, which is crucial for M1 polarization.

DHA suppressed the expression of M2 polarization-related genes and the secretion of associated cytokines

To further dissect the molecular mechanisms by which NLRP12 regulates M1 polarization of macrophages, we compared the expression of M1 and M2-related marker genes in DHA-treated macrophages *in vitro* between shNlrp12-treated and control groups. *Nlrp12* knockdown resulted in a significant reduction in the expression of M1 macrophage marker genes including *CD86* and *CD80*, while M2 macrophage marker genes including Arginase 1 (*Arg1*), *CD206*, transforming growth factor beta (*TGF-β*), *IL-13*, and *IL-10*, were significantly increased in the shNlrp12-treated group compared to that of the shCtrl group (Fig. 4A-G). In addition, guanylate binding protein 5 (GBP5) and inducible nitric oxide synthase (iNOS), known as markers of M1 macrophage, were also

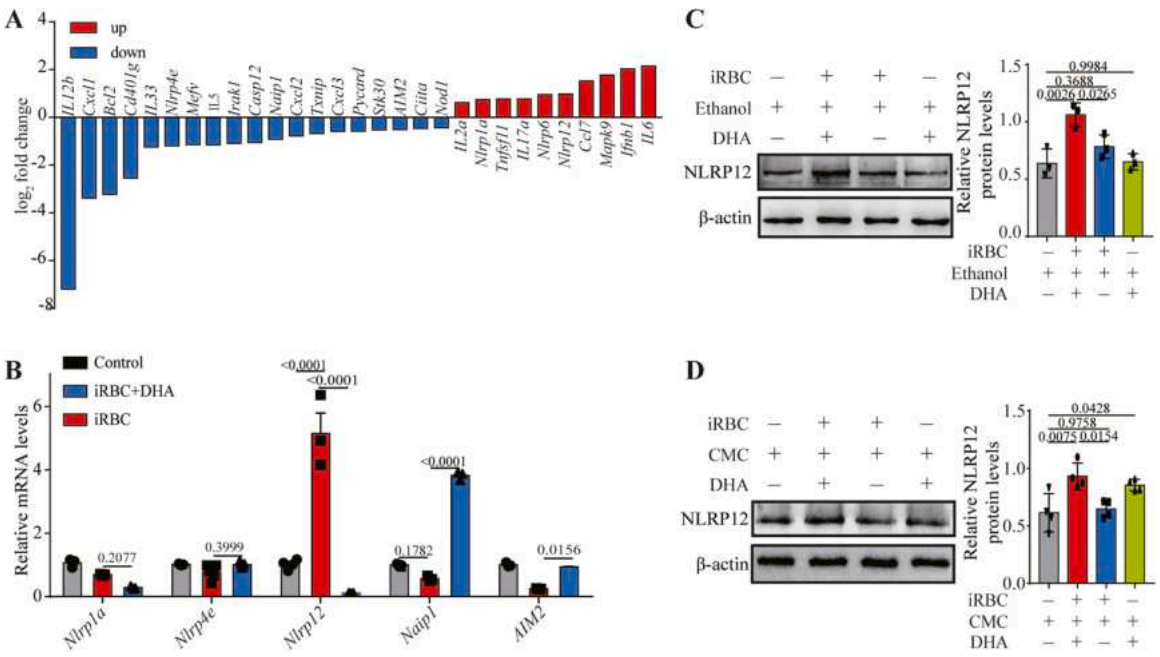

Fig. 2. DHA upregulates NLRP12 expression **(A)** Expression levels of NOD-like receptors (NLRs) in macrophages after DHA treatment. **(B)** Transcription levels of the *Nlrp1a, Nlrp4e, Nlrp12, Naip1*, and *AIM2* genes in macrophages after incubation with iRBCs with or without DHA. **(C)** The expression of NLRP12 in RAW264.7 macrophages was promoted by DHA treatment. **(D)** The expression of NLRP12 in macrophages isolated from mice after DHA treatment. Data represent the mean ± S. E.M., $n \geq 3$. AIM2, absent in melanoma 2; CMC, carboxymethyl cellulose; DHA, dihydroartemisinin; iRBC, infected red blood cells; Naip1, NLR Family Apoptosis Inhibitory Protein; NLRP12, NLR Pyrin Domain Containing 12.

significantly reduced in the shNlrp12 group compared to the shCtrl group (Fig. 4H, I). Furthermore, in the *Nlrp12*-knockdown group, the levels of key pro-inflammatory cytokines associated with M1 macrophages, including IL-12, IL-6, monocyte chemoattractant protein-1 (MCP-1), interferon-γ (IFN-γ), and TNF-α, were significantly suppressed. Conversely, the level of the anti-inflammatory cytokine Il-10, typically secreted by M2 macrophages, was significantly increased (Fig. 4J-O). These results indicated that *Nlrp12* increased DHA-induced M1 polarization and downstream production of cytokines.

The expression of NLRP12 was negatively correlated to that of TSPO

To further delineate the molecular mechanisms by which NLRP12 mediates M1 macrophage polarization, we performed quantitative proteomic analysis to assess protein expression changes in splenic M1 macrophages from shNlrp12- and shCtrl-treated mice. This analysis identified a total of 137 differentially expressed proteins (DEPs) between the two groups, with 83 upregulated and 54 downregulated (Supplementary Fig. 6C). The top 30 DEPs are presented in Supplementary Fig. 6D. Of these, a two-fold rise in TSPO, negatively correlated with the proportion of M1 macrophages, was observed in splenic cells of mice under the treatment of DHA and shNlrp12 lentivirus. Furthermore, the GO analysis showed that these DEPs were enriched in the secretory machinery category including “secretory vesicles”, “secretory granules”, “secretory granule lumen”, “cytoplasmic vesicle lumen”, “vesicle lumen”, and “intermediate filament cells” (Supplementary Fig. 7A). In addition, the DEPs were enriched in functions associated with “programmed cell death” and “the innate immune system" (Supplementary Fig. 7B). The results were further validated using qPCR and Western blotting. Consistent with our proteomic analysis, qPCR validation confirmed that the expression of junction plakoglobin (*Jup*), hematopoietic cell signal transducer (*Hcst*), *Tspo*, BH3 interacting domain death agonist (*Bid*), and NME/NM23 nucleoside diphosphate kinase 2 (*Nme2*) was upregulated in the splenic cells of DHA- and shNlrp12 lentivirus-treated mice. Conversely, the expression of arachidonate lipoxygenase (*Alox*) and *FYVE* and coiled-coil domain autophagy adaptor 1 (Fyco1) was downregulated (Fig. 5A-G). Of these, Western blotting validated that the expression of TSPO and NME2 in DHA treated *Nlrp12* knockdown splenic cells were increased, which was consistent with that of proteomic analysis (Fig. 5H).

To further investigate the role of TSPO in *Nlrp12* knockdown cells, macrophages were treated with a combination of a TSPO-specific inhibitor and DHA. Compared to the solvent control, this combined treatment successfully rescued the M1 macrophage proportion, leading to a renewed increase in M1 cells (Supplementary Fig. 7C, D). These results indicated that TSPO indeed played an inhibitory role in DHA-treated *Nlrp12* knockdown macrophages. Building on our findings that *Nlrp12* knockdown leads to increased TSPO expression, we further investigated their interplay. In *Tspo*-overexpressing macrophages treated with DHA, we observed a significant downregulation of *Nlrp12* expression concomitant with a decrease in M1-polarized macrophages (Fig. 5I-K). Together, these results reveal a negative feedback loop or reciprocal inhibitory relationship between NLRP12 and TSPO, where *Tspo* overexpression suppresses *Nlrp12*, and conversely, *Nlrp12* knockdown upregulates TSPO.

DHA promoted the conversion of classical M1 macrophages into Lcn2^{hi} M1 macrophages

To further differentiate the phenotypes of the macrophages, single-cell RNA sequencing was performed with M1 macrophages separated from the RAW264.7 macrophages after DHA treatment. Transcripts from approximately 74,804 unique genes of 74,798 M1 macrophages were obtained, of these 34,770 cells were from the DHA-treated group and 40,034 from the control group. After quality filtration, transcripts of 73,766 cells were selected for further analysis. The transcripts were categorized in 18 macrophage-clusters based on the expression pattens. The M1 macrophage dataset was chosen for validation, and the clusters were annotated based on the enrichment scores of gene expression profiles (Supplementary Tables 4, 5). The 18 clusters were further divided into 10 cell subsets, including cell proliferation (ubiquitin conjugating enzyme e2 c (Ube2c) and pituitary tumor transforming gene

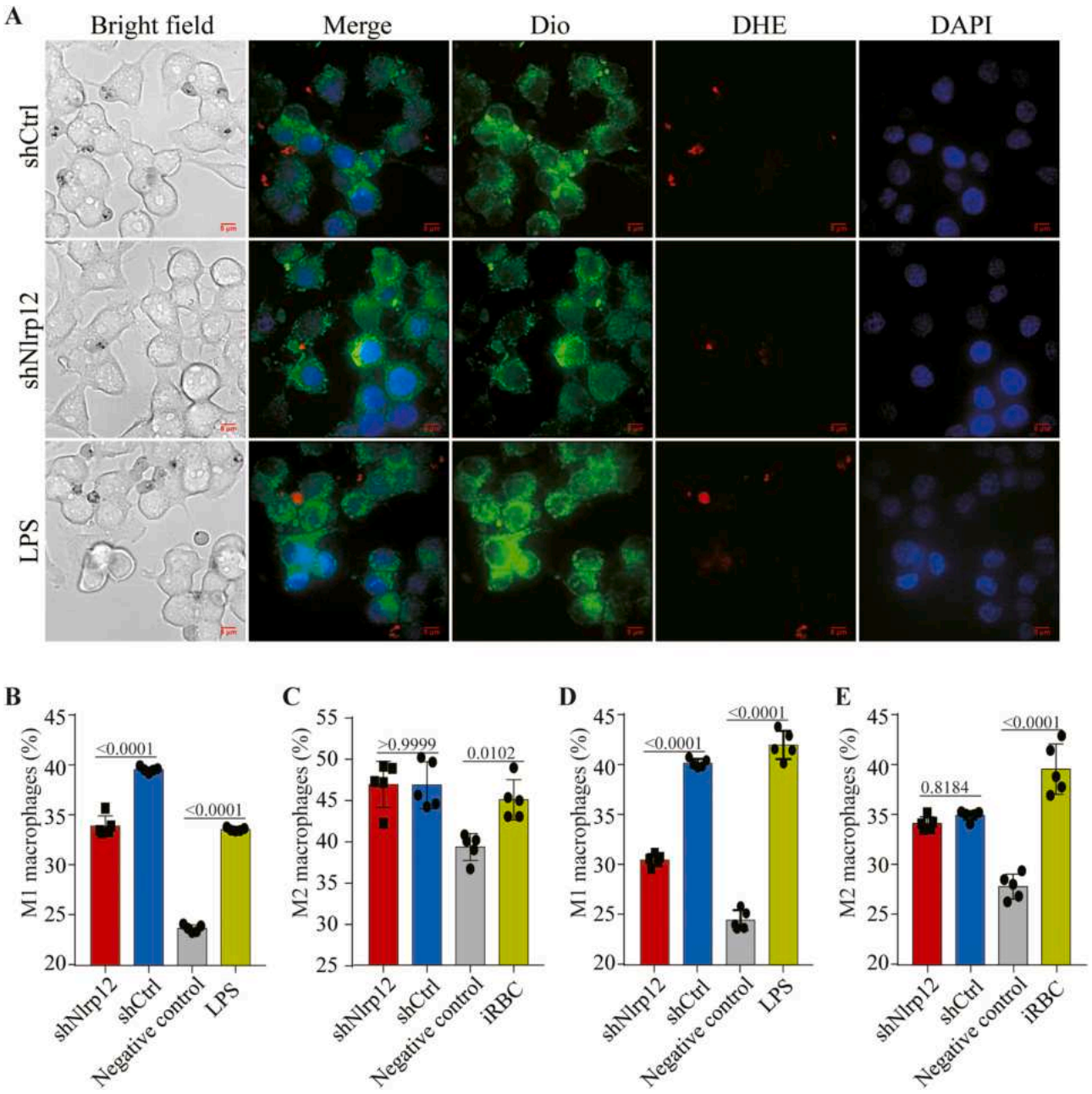

Fig. 3. *Nlrp12* knockdown attenuated the effect of DHA on M1 macrophage polarization. **(A)** Fluorescent labelled iRBCs (red) phagocytosed by shNlrp12-RAW264.7 cells. **(B, C)** Polarization of shNlrp12-knochdoun RAW264.7 cells after DHA treatment compared to the controls. **(D, E)** Macrophage polarization in shNlrp12 knockdown mice after DHA treatment compared to the controls. Data represent the mean ± S.E.M., $n \geq 3$. DAPI, 4′,6-diamidino-2–phenylindole; DHE, dihydroethidium; DiO, dioctadecyloxacarbocyanine perchlorate; iRBC, infected red blood cells; LPS, Lipopolysaccharide.

1 (Pttg1)), inflammation (Lcn2, interleukin 1 receptor antagonist (Il1rn), interferon induced transmembrane protein 3 (Ifitm3)), DHA repair (uracil DNA glycosylase (Ung)), differentiation (acid phosphatase 5 (Acp5)), oxidative stress (predicted gene, 26,917 (Gm26917)), migration and phagocytosis (CD74), and classic M1 macrophages (Supplementary Fig. 8A). DHA treatment significantly increased the proportion of Ung^{hi} macrophages and Lcn2^{hi} M1 macrophages. Meanwhile, Ube2c^{hi} cell proliferation-related M1 macrophages and Acp5^{hi} differentiation-related M1 macrophages were significantly decreased in the DHA groups, while other cell subsets exhibited no significant differences among the four groups (Supplementary Fig. 8B-D). Overall, DHA treatment dramatically increased the polarization of macrophages toward the M1 phenotype, more specifically towards to the Ung^{hi} DNA repair-related and Lcn2^{hi} inflammation-related M1 macrophage subsets. Furthermore, The expression levels of differentiation and inflammation markers including the carbonic anhydrase (*Car6*), SH2 domain containing 6 (*Sh2d6*), *Lcn2*, advillin (*Avil*), the P202b protein (*Ifi202b*), ring finger protein 183 (*Rnf183*), angiopoietin like 6 (*Angptl6*), cytochrome C oxidase subunit 6A2 (*Cox6a2*) and Fc gamma RI (*Fcgr1*), were significantly upregulated in Ung^{hi} macrophages and Lcn2^{hi} inflammation-related M1 macrophages, whereas those of cellular proliferation and cell cycle-related markers, such as the small nucleolar RNA host gene 5 (*Snhg5*), histone cluster 1 H2B family member B (*Hist1h2bb*), *Hist1h2ak, Hist1h1d* and *Hist1h2bl*, were downregulated in Ube2c^{hi} or Acp5^{hi} M1 macrophages after DHA treatment compared to the cells without DHA treatment (Supplementary Fig. 9, 10).

Pseudotime trajectories of Lcn2^{hi} M1 macrophages were reconstructed using the Monocle algorithm, which indicated that they were

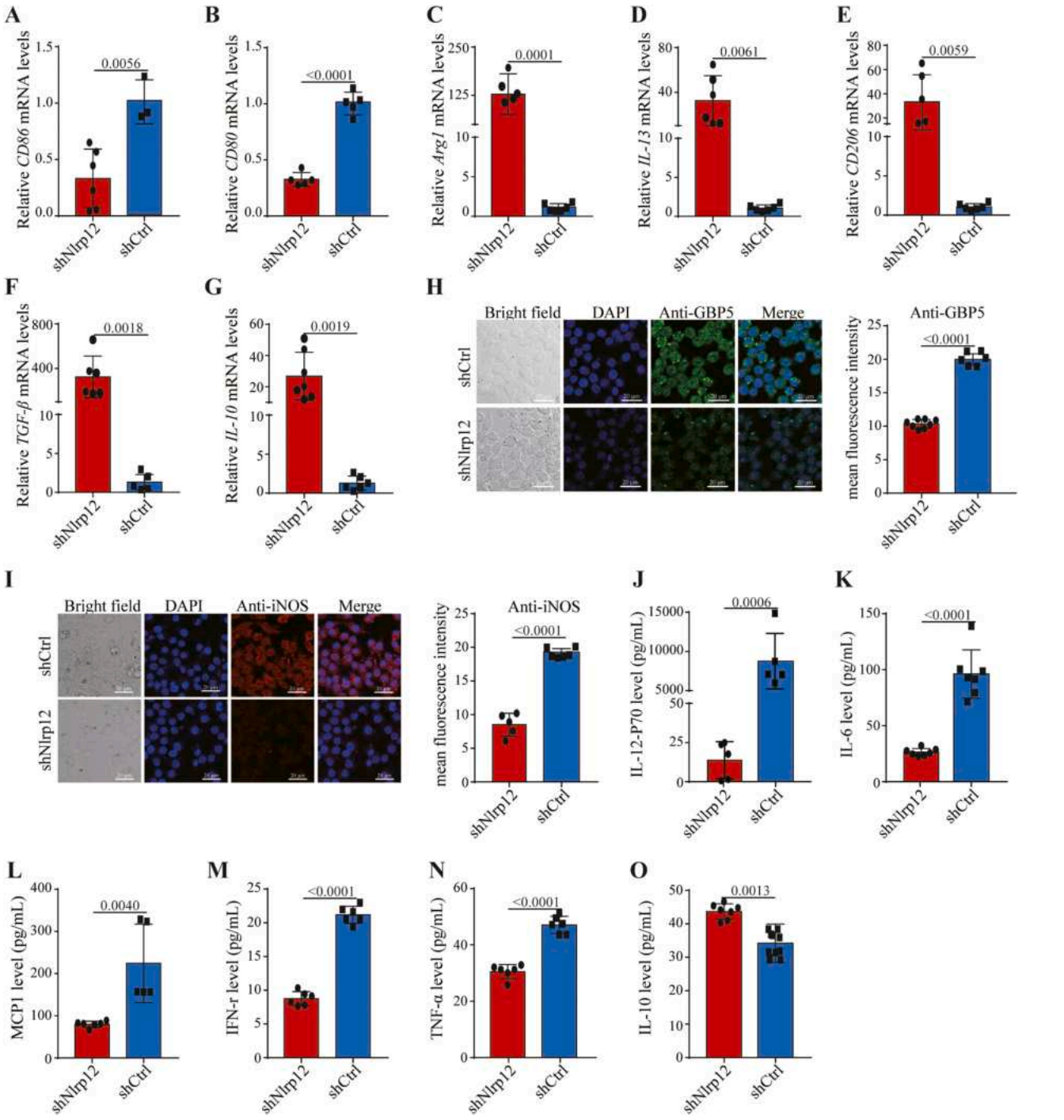

Fig. 4. NLRP12 suppressed the secretion of macrophage-associated cytokines in DHA treated M1macrophage**. (A-G)** Transcription of *CD86, CD80, Arg1, IL-13, CD206, TGF-β* and *IL-10* genes. **(H, I)** The expression of GBP5 and iNOS in RAW264.7 cells. (J-O) Inflammatory cytokine expression level in shNlrp12 and shCtrl group. Data represent the mean ± S.E.M., $n \geq 3$. Arg1, Arginase 1; DAPI, 4′,6-diamidino-2–phenylindole; GBP5, Guanylate Binding Protein 5; IFN-γ, Interferon-γ; IL-13, interleukin-13; iNOS, inducible nitric oxide synthase; TGF-β, Transforming Growth Factor Beta; TNF-α, tumor necrosis factor-α.

derived from classical M1 macrophages (Supplementary Fig. 11). The expression of gene modules associated with cellular proliferation gradually decreased from early pseudo-time and significantly dropped at late pseudo-time, including centromere protein F (*Cenpf*), *Ube2c*, cell division cycle associated 8 (*Cdca8*), tubulin beta 4B Class IVb (*Tubb4b*), protein regulator of cytokinesis 1 (*Prc1*), and polo like kinase 1 (*Plk1*) (Supplementary Fig.12A). Conversely, the expression of gene modules linked to inflammation and immunity steadily increased from early pseudo-time and peaked at late pseudo-time, including *Lcn2*, peroxiredoxin 1 (*Prdx1*), *Car6*, C-X-C motif chemokine ligand 2 (*Cxcl2*), secreted phosphoprotein 1 (*Spp1*), and glyceraldehyde-3-phosphate dehydrogenase (*Gapdh*) (Supplementary Fig. 12B). Genes whose expression was upregulated in M1 macrophages transitioning into $Lcn2^{hi}$ M1 macrophages were primarily enriched in Fc gamma R-mediated phagocytosis, Foxo signaling, and IL-17 signaling, which facilitate M1 function (Supplementary Fig. 13A). Regulation of histone H3-K9 acetylation, positive regulation of macrophage cytokine production, immunoglobulin generation, and oxidoreductase activity were also enriched in GO analysis (Supplementary Fig. 13B). CellphoneDB analysis indicated $Lcn2^{hi}$ M1 macrophages showed stronger interactions

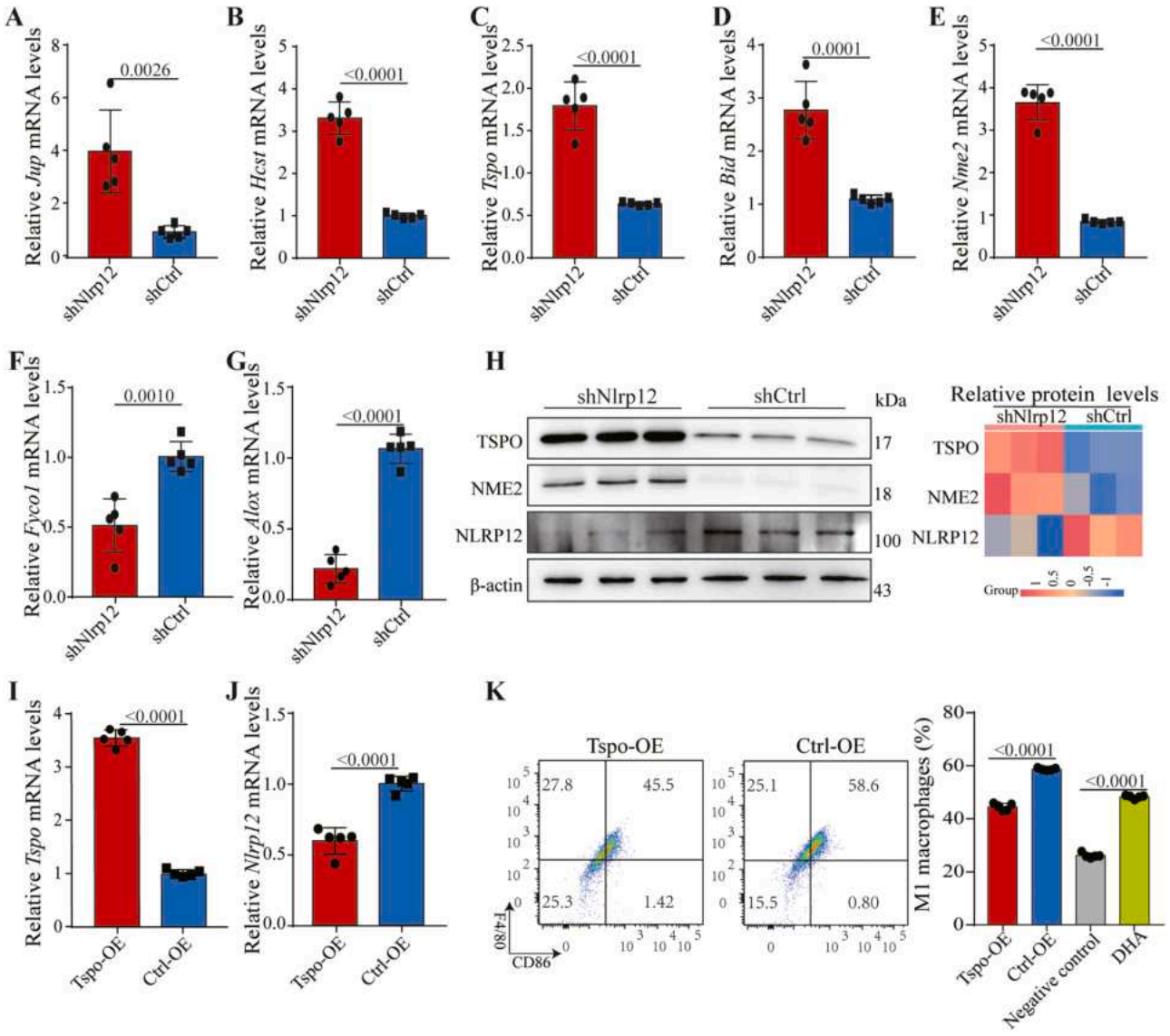

Fig. 5. NLRP12 inhibited the expression of TSPO in DHA treated M1 macrophages**. (A-G)** The transcription of *Jup, Hcst, Tspo, Bid, Nme2, Fyco1*, and *Alox* genes. **(H)** The expression of TSPO, NME2, and NLRP12. **(I)** The transcription *Tspo* gene. **(J)** The transcription of *Nlrp12* gene. **(K)** Polarization of Tspo-OE-RAW264.7 cells toward M1 phenotypes. Data represent the mean ± S.E.M., $n \geq 3$. Alox, Arachidonate Lipoxygenase; Bid, BH3 Interacting Domain Death Agonist; DHA, dihydroartemisinin; Fyco1, FYVE And Coiled-Coil Domain Autophagy Adaptor 1; Hcst, Hematopoietic Cell Signal Transducer; Jup, Junction Plakoglobin; NLRP12, NLR Pyrin Domain Containing 12; Nme2, NME/NM23 Nucleoside Diphosphate Kinase 2; TSPO, translocator protein.

with other M1 macrophages in the DHA treatment group compared to that of the control group (Supplementary Fig. 14A, B). Lcn2^{hi} M1 macrophages could directly contact other M1 macrophages through ligand–receptor pairs, namely, *Spp1-Cd44, C5ar1-Rps19*, and *Cd74- Mif*, which induce pro-inflammatory M1 macrophage differentiation (Supplementary Fig. 14 A, B). Additionally, genes whose expression was upregulated in Ube2c^{hi} M1 macrophages were primarily enriched in cell cycle, cellular senescence, and mitophagy (Supplementary Fig. 13C). Moreover, the transcription, DNA-templated and RNA biosynthetic process terms were also enriched in the GO analysis (Supplementary Fig. 13D). The transcriptomic data coupled with CellphoneDB analysis suggested that Ube2c ^{hi} M1 macrophages could directly contact other M1 macrophages through *Lrp6-Cklf*, which is essential for cell proliferation (Supplementary Fig. 14C, D). Overall, DHA treatment promoted interactions of Lcn2^{hi} M1 macrophages with other macrophages, which induce pro-inflammatory M1 differentiation.

Discussion

Macrophages serve as key cellular mediators in host defense against *Plasmodium* infection (Kapralov et al., 2020). DHA, the most widely used antimalarial drug, has been reported to possess immunomodulatory properties and exhibited efficacy in treatment of various autoimmune diseases, including systemic lupus erythematosus and rheumatoid arthritis (Li et al., 2022). In this study, DHA was found to promote M1 type macrophages polarization and their phagocytosis against *Plasmodium*-infected erythrocytes (Video 1, 2, Fig. 1A-E; Supplementary Fig. 3C). PCR-array based analysis revealed a significant NLRP12 upregulation in macrophages after exposure to DHA compared to that of the control cells (Fig. 2A-D; Supplementary Fig. 3D). Knocking-down *Nlrp12* in both cell lines and cells isolated from mouse spleen confirmed its positive association with M1 macrophage polarization in responses to DHA treatment (Fig. 3, 4). Proteomic analysis showed that DHA treatment significantly suppressed TSPO expression in M1 macrophages sorted from the *Nlrp12* knockdown mice (Fig. 5). Furthermore,

to determine if heterogeneity existed in DHA-induced M1 macrophages, scRNA-sequencing was used to categorize the cell populations of the DHA treated macrophages and the untreated control. The results showed that DHA treatment promoted the conversion of classical M1 macrophages into Lcn2^{hi} M1 macrophages (Supplementary Fig. 8–14). Overall, our results indicated that DHA promoted macrophage M1 polarization through the NLRP12-TSPO axis, reflecting a DHA-enhanced adaptive immune response against parasites (Fig. 5).

An important mechanism of malarial parasite clearance is phagocytosis of iRBCs by macrophages (Langhorne et al., 2008). Of these, M1 macrophages, which form a crucial front line against *Plasmodium* infection, exhibit high levels of phagocytic activity (Singh et al., 2020). In this study, DHA promoted macrophage polarization toward the M1 phenotype and significantly enhanced the phagocytic capacity of macrophages both *in vitro* and *in vivo* (Fig. 1).

Inflammasome NLR family members, such as PAMP sensors, stimulate macrophage polarization upon activation (Rao et al., 2022b; Wong et al., 2018). In this study, the NLRP12 expression was significantly increased in M1 macrophages after DHA treatment (Fig. 2A-D; Supplementary Fig. 3D). Consistently, the *Nlrp12* knockdown significantly reduced the proportion of M1 macrophages (Fig. 3), which was likely due to the downregulation of M1 marker gene (*CD86* and *CD80*) and protein (GBP5 and iNOS) expression and upregulation of M2 marker genes (*Argl, CD206*, and *TGF-β*) (Fig. 4A-I) in the *Nlrp12* knockdown cells. This indicated that DHA could induce macrophage M1 polarization by increasing NLRP12 expression. However, the molecular pathways involved in DHA-induced NLRP12 activation will be further explored.

Previous studies indicate that hemozoin can partially reverse the M2-like phenotype activation in human monocytes by artemisinin (ART) (Bobade et al., 2019). In inflammatory bowel disease, there is an increase in M1 macrophages. However, ART can drive macrophages towards the M2 phenotype, improving colitis (Huai et al., 2021). This highlights the ability of ART to modulate macrophage phenotypes. Macrophages serve as a "factory" for the activation and expression of inflammasomes, including NLRP12. In mouse models of pneumonia, increased expression of NLRP12 in lung macrophages has been shown to be critical for host survival, bacterial clearance, and neutrophil recruitment during pneumonia treatment (Cai et al., 2016). Similarly, NLRP12 has been reported to enhance macrophage immune responses and alleviate symptoms in the treatment of herpes simplex keratitis (Jiang et al., 2024). Macrophage polarization from M2 to M1 was induced by DHA treatment in *Plasmodium*-infected mice, which was closely associated with upregulated expression of NLRP12 in these macrophages. These data demonstrate that DHA regulates macrophage polarization by promoting NLRP12 expression, thereby enhancing the immune response against malaria.

TSPO, formerly known as the peripheral benzodiazepine receptor, is a mitochondrial outer membrane protein ubiquitously expressed in peripheral tissues (Selvaraj and Stocco, 2015). TSPO overexpression suppressed the LPS-induced macrophage M1 polarization (Horiguchi et al., 2019; Orecchioni et al., 2019). This evidence indicated that TSPO is a negative regulator in M1-macrophage polarization. Through quantitative proteomic analysis, the expression of TSPO was found significantly increased in the plenic M1 macrophages of *Nlrp12* knockdown mice infected with *P. berghei,* while DHA treatment can reverse the effect. qPCR and Western blotting verified above result (Fig. 5). These findings suggested that DHA can suppress the expression of TSPO by upregulation of NLRP12 in the M1 macrophages. Furthermore, scRNA-seq analysis revealed DHA promoted the conversion of classical M1 macrophages into Lcn2^{hi} and Ube2c^{hi} M1 macrophages, which is in line to the previous finding that upregulation of Lcn2 in macrophages is a critical factor in controlling malaria infections (Zhao et al., 2012). Further, the ability of M1 macrophage-derived exosomes to deliver Lcn2 suggests a potential mechanism for amplifying these protective effects (Fan et al., 2024). These multifaceted functions of Lcn2^{hi} M1 macrophages underscore their importance in malaria control.

Overall, this study revealed DHA is not only a potent antimalarial but also an immunomodulator. DHA preferentially drives macrophages towards M1 type polarization, which is closely associated with cellular immune reaction to malaria (Supplementary Fig. 15).

Conclusions

In summary, our study elucidates the pivotal role of DHA in promoting M1 macrophage polarization to enhance immune responses against *Plasmodium* infection. This polarization is closely associated with the upregulation of *Nlrp12* expression in macrophages after exposure to DHA, as evidenced by PCR-array analysis and confirmed through *Nlrp12* knockdown experiments in both cell lines and macrophages isolated from mouse spleens. Further proteomic analysis revealed that DHA treatment leads to a substantial decrease in TSPO expression in macrophages derived from *Nlrp12*-deficient mice, highlighting the critical involvement of the NLRP12-TSPO axis in this regulatory pathway. Additionally, scRNA-seq provided insights into the cellular heterogeneity induced by DHA treatment, revealing a transition from classical M1 macrophages to Lcn2^{hi} M1 macrophages. This shift underscores DHA's ability to enhance the adaptive immune response, ensuring a more effective clearance of malaria parasites.

Data availability

All data supporting the findings of this study are available on paper. Source data are provided in the Supplementary materials.

CRediT authorship contribution statement

Xin Li: Writing – original draft, Methodology, Investigation, Formal analysis, Data curation. **Qilong Li:** Writing – original draft, Validation, Methodology, Investigation, Formal analysis. **Ning Jiang:** Validation, Supervision, Resources, Project administration. **Kexin Zheng:** Visualization, Methodology, Investigation. **Yiwei Zhang:** Methodology, Investigation. **Xiaoyu Sang:** Methodology, Investigation. **Ying Feng:** Visualization, Methodology. **Ran Chen:** Visualization. **Qijun Chen:** Writing – review & editing, Supervision, Resources, Project administration, Funding acquisition, Conceptualization.

Declaration of competing interest

The authors declare that they have no competing or financial interests that could have appeared to influence the work reported in this manuscript.

Acknowledgments

This research was supported the National Nature and Science Foundation of China (grant number 82030060) to Q.C., and the CAMS Innovation Fund for Medical Sciences (CIFMS) (grant number 2019-I2M-5-042) to N.J.

Supplementary materials

Supplementary material associated with this article can be found, in the online version, at doi:10.1016/j.phymed.2025.156913.

References

Asahi, H., Niikura, M., Inoue, S.-I., Sendo, F., Kobayashi, F., Wada, A., 2023. Dihydroartemisinin disrupts zinc homeostasis in *plasmodium* falciparum to potentiate its antimalarial action *via* pyknosis. ACS Infect. Dis. 9, 1303–1309. https://doi.org/10.1021/acsinfecdis.3c00031.

Bobade, D., Khandare, A.V., Deval, M., Shastry, P., Deshpande, P., 2019. Hemozoin-induced activation of human monocytes toward M2-like phenotype is partially

reversed by antimalarial drugs-chloroquine and artemisinin. Microbiologyopen 8, e00651. https://doi.org/10.1002/mbo3.651.
Cai, S., Batra, S., Piero, F.D., Jeyaseelan, S., 2016. NLRP12 modulates host defense through IL-17A-CXCL1 axis. Mucosal. Immunol. 9, 503–514. https://doi.org/10.1038/mi.2015.80.
Caronni, N., La Terza, F., Vittoria, F.M., Barbiera, G., Mezzanzanica, L., Cuzzola, V., Barresi, S., Pellegatta, M., Canevazzi, P., Dunsmore, G., Leonardi, C., Montaldo, E., Lusito, E., Dugnani, E., Citro, A., Ng, M.S.F., Schiavo Lena, M., Drago, D., Andolfo, A., Brugiapaglia, S., Scagliotti, A., Mortellaro, A., Corbo, V., Liu, Z., Mondino, A., Dellabona, P., Piemonti, L., Taveggia, C., Doglioni, C., Cappello, P., Novelli, F., Iannacone, M., Ng, L.G., Ginhoux, F., Crippa, S., Falconi, M., Bonini, C., Naldini, L., Genua, M., Ostuni, R., 2023. IL-1β^{+} macrophages fuel pathogenic inflammation in pancreatic cancer. Nature 623, 415–422. https://doi.org/10.1038/s41586-023-06685-2.
Coban, C., Ishii, K.J., Kawai, T., Hemmi, H., Sato, S., Uematsu, S., Yamamoto, M., Takeuchi, O., Itagaki, S., Kumar, N., Horii, T., Akira, S., 2005. Toll-like receptor 9 mediates innate immune activation by the malaria pigment hemozoin. J. Exp. Med. 201, 19–25. https://doi.org/10.1084/jem.20041836.
Fan, C., Wang, Wei, Yu, Z., Wang, J., Xu, W., Ji, Z., He, W., Hua, D., Wang, Wentao, Yao, L., Deng, Y., Geng, D., Wu, X., Mao, H., 2024. M1 macrophage-derived exosomes promote intervertebral disc degeneration by enhancing nucleus pulposus cell senescence through LCN2/NF-κb signaling axis. J. Nanobiotechnol. 22, 301. https://doi.org/10.1186/s12951-024-02556-8.
Gazzinelli, R.T., Kalantari, P., Fitzgerald, K.A., Golenbock, D.T., 2014. Innate sensing of malaria parasites. Nat. Rev. Immunol. 14, 744–757. https://doi.org/10.1038/nri3742.
Gibbons, P.L., Batty, K.T., Barrett, P.H.R., Davis, T.M.E., Ilett, K.F., 2007. Development of a pharmacodynamic model of murine malaria and antimalarial treatment with dihydroartemisinin. Int J Parasitol 37, 1569–1576. https://doi.org/10.1016/j.ijpara.2007.05.001.
Guo, H., Callaway, J.B., Ting, J.P.-Y., 2015. Inflammasomes: mechanism of action, role in disease, and therapeutics. Nat. Med. 21, 677–687. https://doi.org/10.1038/nm.3893.
Horiguchi, Y., Ohta, N., Yamamoto, S., Koide, M., Fujino, Y., 2019. Midazolam suppresses the lipopolysaccharide-stimulated immune responses of human macrophages *via* translocator protein signaling. Int Immunopharmacol 66, 373–382. https://doi.org/10.1016/j.intimp.2018.11.050.
Huai, M., Zeng, J., Ge, W., 2021. Artemisinin ameliorates intestinal inflammation by skewing macrophages to the M2 phenotype and inhibiting epithelial–mesenchymal transition. Int. Immunopharmacol. 91, 107284. https://doi.org/10.1016/j.intimp.2020.107284.
Jiang, J., Zhang, D., Liu, W., Yang, J., Yang, F., Liu, J., Hu, K., 2024. Overexpression of NLRP12 enhances macrophage immune response and alleviates herpes simplex keratitis. Front Cell Infect Microbiol. 14, 1416105. https://doi.org/10.3389/fcimb.2024.1416105.
Jiao, Y., Zhang, T., Zhang, C., Ji, H., Tong, X., Xia, R., Wang, W., Ma, Z., Shi, X., 2021. Exosomal miR-30d-5p of neutrophils induces M1 macrophage polarization and primes macrophage pyroptosis in sepsis-related acute lung injury. Crit. Care 25, 356. https://doi.org/10.1186/s13054-021-03775-3.
Kalantari, P., DeOliveira, R.B., Chan, J., Corbett, Y., Rathinam, V., Stutz, A., Latz, E., Gazzinelli, R.T., Golenbock, D.T., Fitzgerald, K.A., 2014. Dual engagement of the NLRP3 and AIM2 inflammasomes by *plasmodium*-derived hemozoin and DNA during malaria. Cell Rep. 6, 196–210. https://doi.org/10.1016/j.celrep.2013.12.014.
Kapralov, A.A., Yang, Q., Dar, H.H., Tyurina, Y.Y., Anthonymuthu, T.S., Kim, R., St Croix, C.M., Mikulska-Ruminska, K., Liu, B., Shrivastava, I.H., Tyurin, V.A., Ting, H.-C., Wu, Y.L., Gao, Y., Shurin, G.V., Artyukhova, M.A., Ponomareva, L.A., Timashev, P.S., Domingues, R.M., Stoyanovsky, D.A., Greenberger, J.S., Mallampalli, R.K., Bahar, I., Gabrilovich, D.I., Bayır, H., Kagan, V.E., 2020. Redox lipid reprogramming commands susceptibility of macrophages and microglia to ferroptotic death. Nat Chem Biol 16, 278–290. https://doi.org/10.1038/s41589-019-0462-8.
Langhorne, J., Ndungu, F.M., Sponaas, A.-M., Marsh, K., 2008. Immunity to malaria: more questions than answers. Nat. Immunol. 9, 725–732. https://doi.org/10.1038/ni.f.205.
Li, Q., Yuan, Q., Jiang, N., Zhang, Y., Su, Z., Lv, L., Sang, X., Chen, R., Feng, Y., Chen, Q., 2022. Dihydroartemisinin regulates immune cell heterogeneity by triggering a cascade reaction of CDK and MAPK phosphorylation. Signal. Transduct. Target. Ther. 7, 222. https://doi.org/10.1038/s41392-022-01028-5.
Liu, T., Wang, L., Liang, P., Wang, X., Liu, Y., Cai, J., She, Y., Wang, D., Wang, Z., Guo, Z., Bates, S., Xia, X., Huang, J., Cui, J., 2021. USP19 suppresses inflammation and promotes M2-like macrophage polarization by manipulating NLRP3 function *via* autophagy. Cell. Mol. Immunol. 18, 2431–2442. https://doi.org/10.1038/s41423-020-00567-7.
Orecchioni, M., Ghosheh, Y., Pramod, A.B., Ley, K., 2019. Macrophage polarization: different gene signatures in M1(LPS+) *vs.* classically and M2(LPS-) *vs.* alternatively activated macrophages. Front Immunol. 10, 1084. https://doi.org/10.3389/fimmu.2019.01084.
Pereira, L.M.N., Assis, P.A., de Araújo, N.M., Durso, D.F., Junqueira, C., Ataíde, M.A., Pereira, D.B., Lien, E., Fitzgerald, K.A., Zamboni, D.S., Golenbock, D.T., Gazzinelli, R.T., 2020. Caspase-8 mediates inflammation and disease in rodent malaria. Nat. Commun. 11, 4596. https://doi.org/10.1038/s41467-020-18295-x.
Rao, S.D., Chen, Q., Wang, Q., Orth-He, E.L., Saoi, M., Griswold, A.R., Bhattacharjee, A., Ball, D.P., Huang, H.-C., Chui, A.J., Covelli, D.J., You, S., Cross, J.R., Bachovchin, D. A., 2022a. M24B aminopeptidase inhibitors selectively activate the CARD8 inflammasome. Nat. Chem. Biol. 18, 565–574. https://doi.org/10.1038/s41589-021-00964-7.
Rao, X., Zhou, X., Wang, G., Jie, X., Xing, B., Xu, Y., Chen, Y., Li, J., Zhu, K., Wu, Z., Wu, G., Wu, C., Zhou, R., 2022b. NLRP6 is required for cancer-derived exosome-modified macrophage M2 polarization and promotes metastasis in small cell lung cancer. Cell Death Dis. 13, 891. https://doi.org/10.1038/s41419-022-05336-0.
Schroder, K., Tschopp, J., 2010. The inflammasomes. Cell 140, 821–832. https://doi.org/10.1016/j.cell.2010.01.040.
Selvaraj, V., Stocco, D.M., 2015. The changing landscape in translocator protein (TSPO) functions. Trends Endocrinol. Metab. 26, 341–348. https://doi.org/10.1016/j.tem.2015.02.007.
Singh, K.S., Leu, J.I.-J., Barnoud, T., Vonteddu, P., Gnanapradeepan, K., Lin, C., Liu, Q., Barton, J.C., Kossenkov, A.V., George, D.L., Murphy, M.E., Dotiwala, F., 2020. African-centric TP53 variant increases iron accumulation and bacterial pathogenesis but improves response to malaria toxin. Nat. Commun. 11, 473. https://doi.org/10.1038/s41467-019-14151-9.
Sundaram, B., Pandian, N., Mall, R., Wang, Y., Sarkar, R., Kim, H.J., Malireddi, R.K.S., Karki, R., Janke, L.J., Vogel, P., Kanneganti, T.-D., 2023. NLRP12-PANoptosome activates PANoptosis and pathology in response to heme and PAMPs. Cell 186, 2783–2801.e20. https://doi.org/10.1016/j.cell.2023.05.005.
Venkatesan, P., 2024. The 2023 WHO World malaria report. Lancet Microbe. 5, e214. https://doi.org/10.1016/S2666-5247(24)00016-8.
Wallender, E., Ali, A.M., Hughes, E., Kakuru, A., Jagannathan, P., Muhindo, M.K., Opira, B., Whalen, M., Huang, L., Duvalsaint, M., Legac, J., Kamya, M.R., Dorsey, G., Aweeka, F., Rosenthal, P.J., Savic, R.M., 2021. Identifying an optimal dihydroartemisinin-piperaquine dosing regimen for malaria prevention in young Ugandan children. Nat. Commun. 12, 6714. https://doi.org/10.1038/s41467-021-27051-8.
White, N.J., 2008. Qinghaosu (artemisinin): the price of success. Science 320, 330–334. https://doi.org/10.1126/science.1155165.
Wong, D.W.L., Yiu, W.H., Chan, K.W., Li, Y., Li, B., Lok, S.W.Y., Taketo, M.M., Igarashi, P., Chan, L.Y.Y., Leung, J.C.K., Lai, K.N., Tang, S.C.W., 2018. Activated renal tubular wnt/β-catenin signaling triggers renal inflammation during overload proteinuria. Kidney. Int. 93, 1367–1383. https://doi.org/10.1016/j.kint.2017.12.017.
Zhang, T., Zhang, Y., Jiang, N., Zhao, X., Sang, X., Yang, N., Feng, Y., Chen, R., Chen, Q., 2020. Dihydroartemisinin regulates the immune system by promotion of $CD8^{+}$ T lymphocytes and suppression of B cell responses. Sci. China Life Sci. 63, 737–749. https://doi.org/10.1007/s11427-019-9550-4.
Zhao, H., Konishi, A., Fujita, Y., Yagi, M., Ohata, K., Aoshi, T., Itagaki, S., Sato, S., Narita, H., Abdelgelil, N.H., Inoue, M., Culleton, R., Kaneko, O., Nakagawa, A., Horii, T., Akira, S., Ishii, K.J., Coban, C., 2012. Lipocalin 2 bolsters innate and adaptive immune responses to blood-stage malaria infection by reinforcing host iron metabolism. Cell Host Microbe. 12, 705–716. https://doi.org/10.1016/j.chom.2012.10.010.